Electronic Supplementary Information

Synthesis of mesoporous Fe_3Si aerogel as a photo-thermal material for highly efficient and stable corrosive-water evaporation

Fengyu Zhang,[a] *Yaguang Li,*[*a] *Xianhua Bai,*[a] *Shufang Wang,*[a] *Baolai Liang,*[a] *Guangsheng Fu,*[a] *Zhong-Shuai Wu*[*b]

a Hebei Key Lab of Optic-electronic Information and Materials, The College of Physics Science and Technology, Hebei University, Baoding, 071002, China.

b Dalian National Laboratory for Clean Energy, Dalian Institute of Chemical Physics, Chinese Academy of Sciences, 457 Zhongshan Road, Dalian 116023, China.

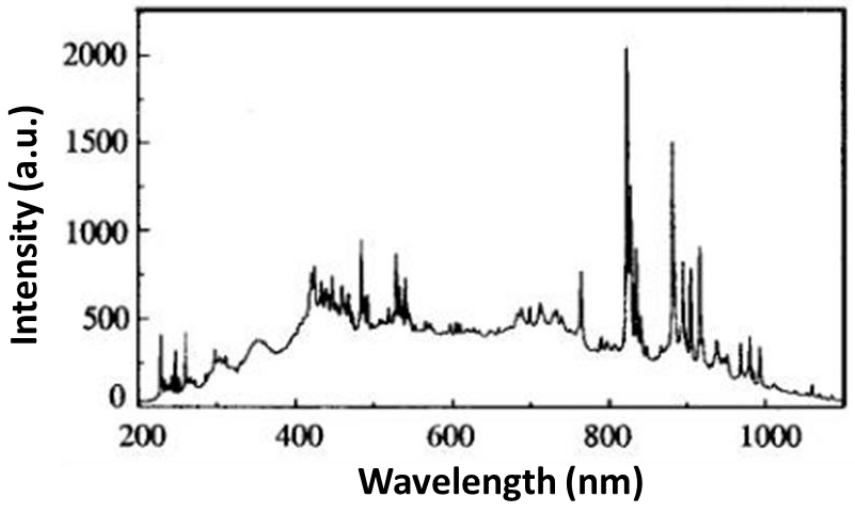

Figure S1. The emission spectrum of xenon lamp provided by perfectlight Co., Ltd.

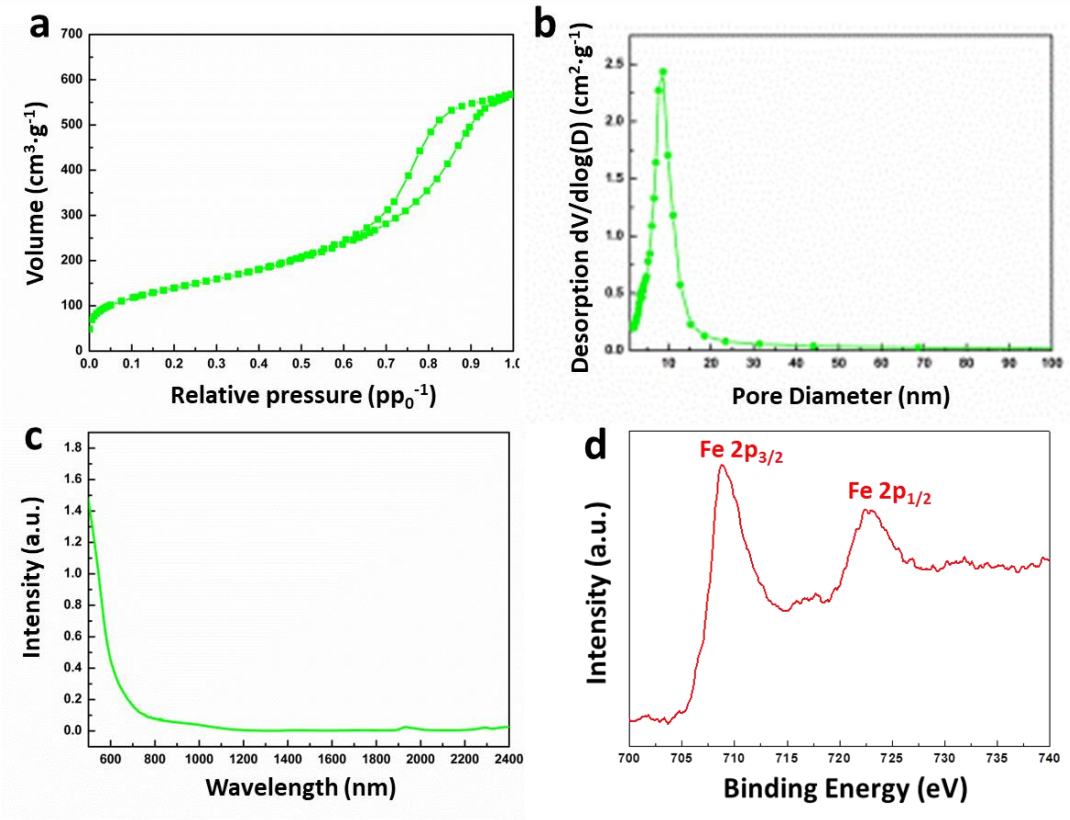

Figure S2. (a) Nitrogen adsorption and desorption isotherm, (b) pore size distribution (c) ultraviolet-Visible-Near Infrared absorption spectrum, (d) Fe 2p XPS spectrum of Fe-doped SiO_2 aerogel.

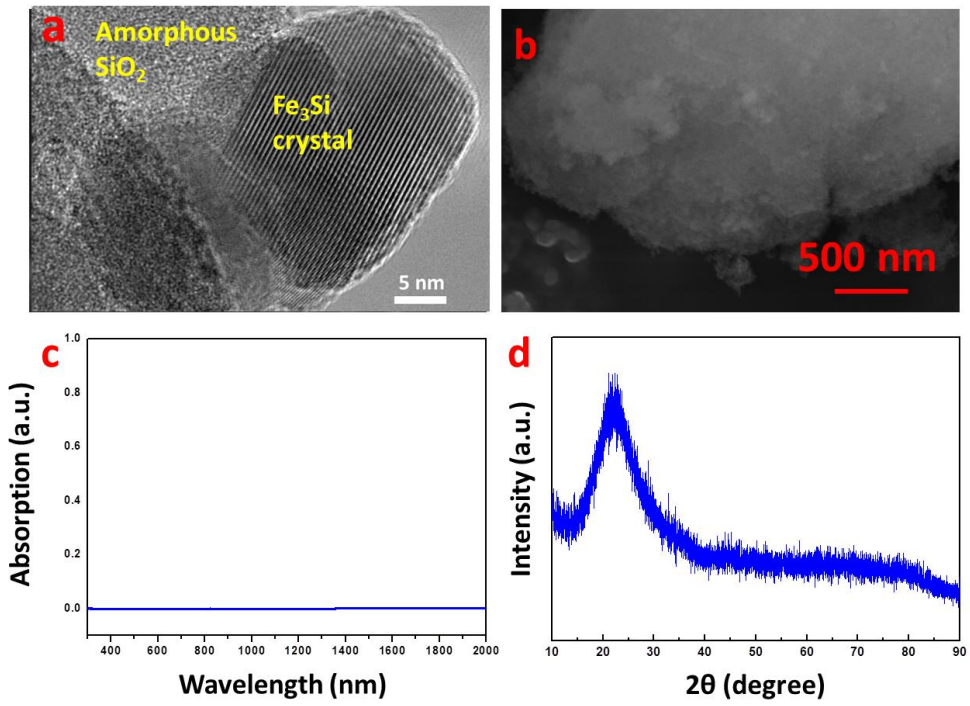

Figure S3. (a) HRTEM image of the interface between Fe_3Si crystal and amorphous SiO_2 in Fe_3Si aerogel. (b) SEM image, (c) ultraviolet-visible-near infrared absorption spectrum, (d) XRD pattern of SiO_2 aerogel.

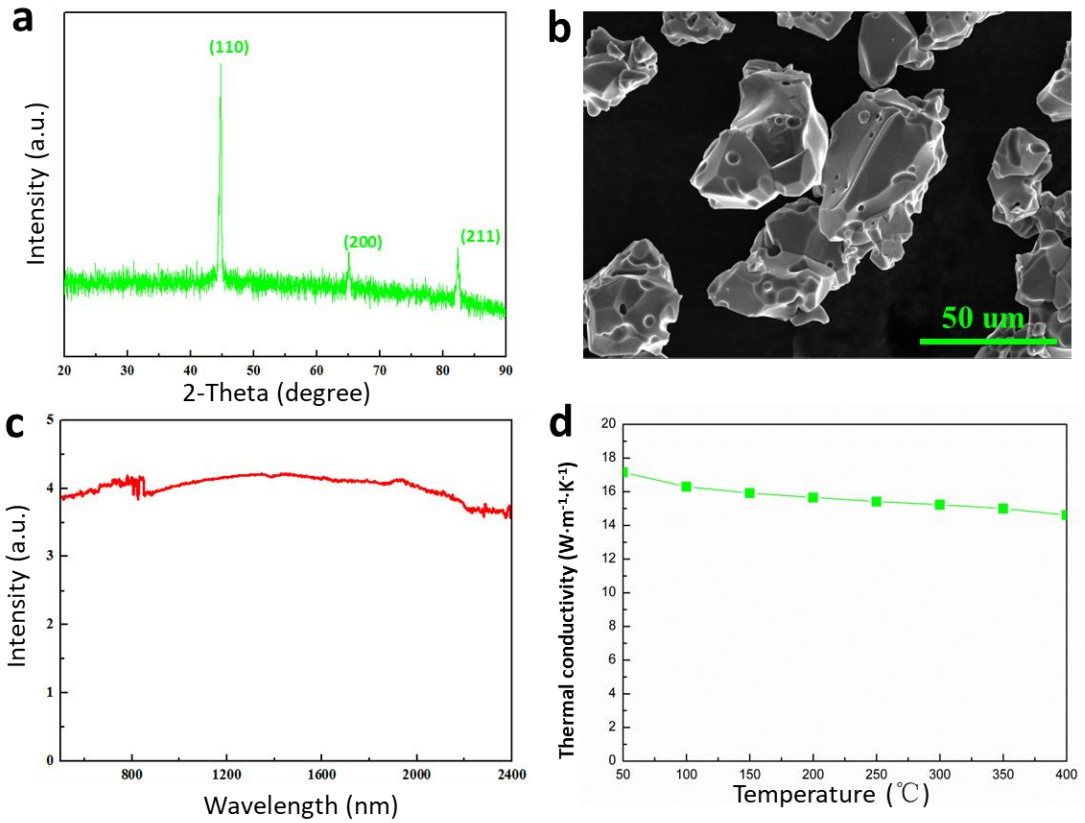

Figure S4. (a) XRD pattern, (b) SEM image, (c) ultraviolet-visible-near infrared absorption spectrum, (d) temperature-dependent total thermal conductivity of pure bulk Fe_3Si particles.

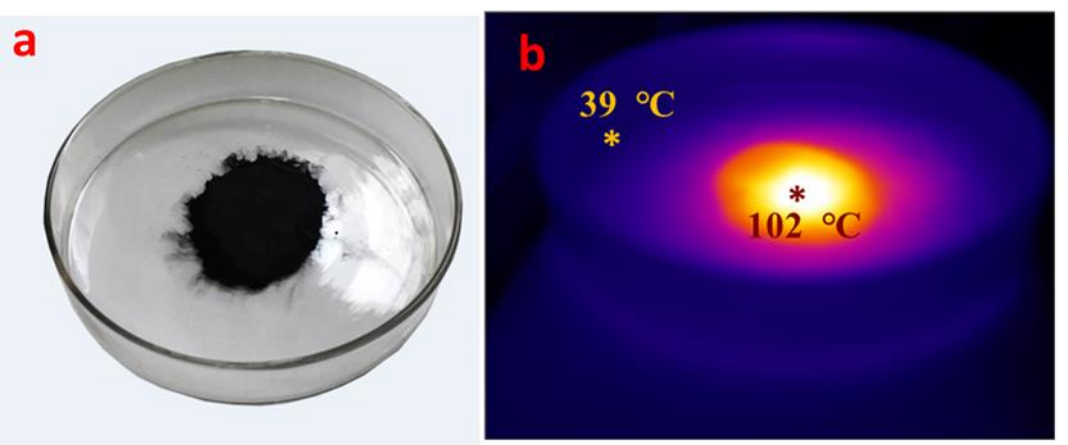

Figure S5. (a) Photograph of Fe_3Si aerogel loaded in a glass dish, (b) the corresponding infra-red (IR) image with the irradiation of 1 kW m^{-2} standard sunlight obtained by IR camera.

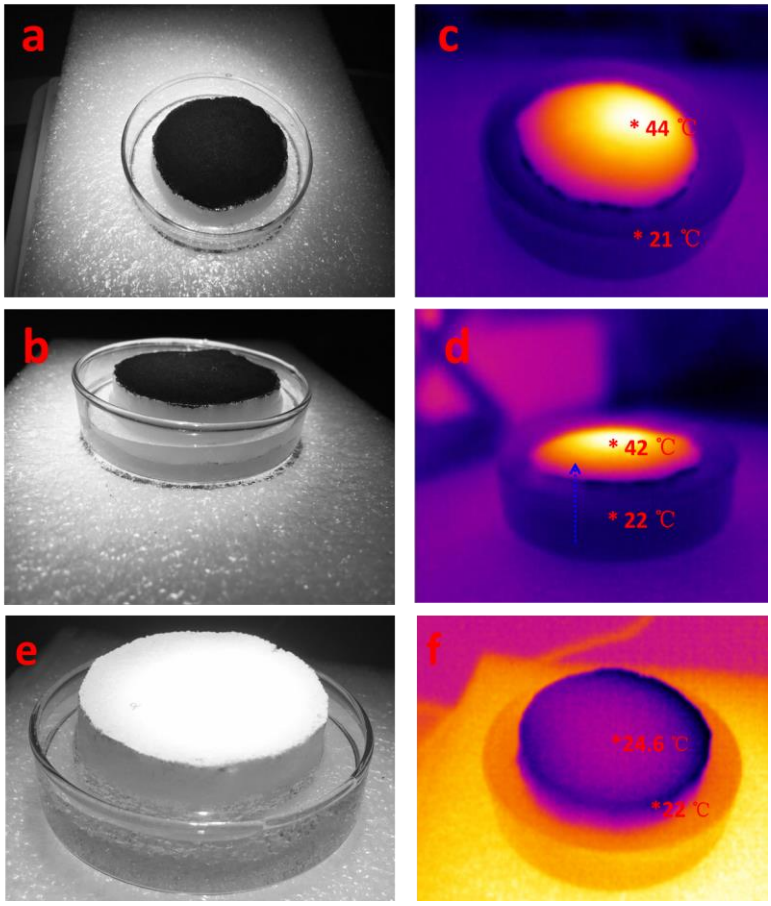

Figure S6. (a,b) Photographs and (c,d) corresponding top-view and side-view IR images of bulk Fe_3Si aerogel supported on melamine foam in solar-vapor desalination unit after 10 minutes of 1.0 kw·m^{-2} sunlight illumination. (e) Photograph and (f) IR image of SiO_2 aerogel supported on melamine foam in solar-vapor desalination unit after 10 minutes of 1.0 kw·m^{-2} sunlight illumination.

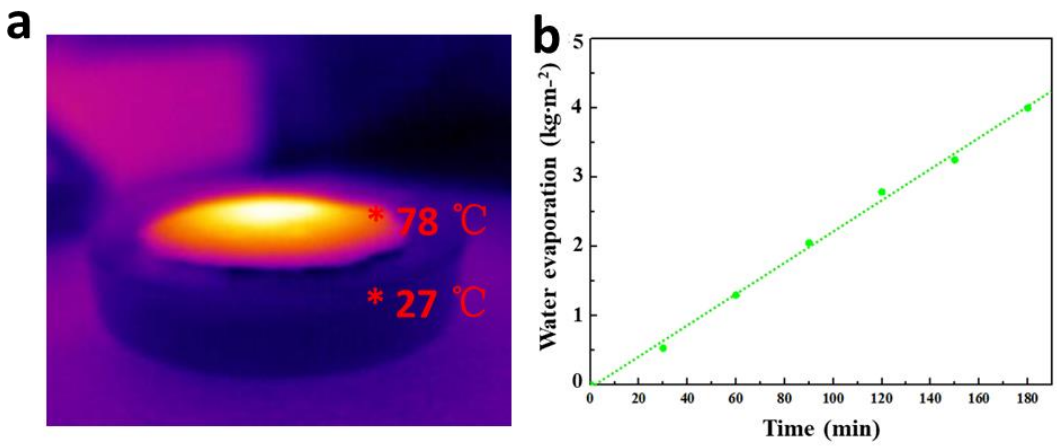

Figure S7. (a) Infrared (IR) image (obtained by IR camera) of hydrophobic Fe_3Si aerogel/melamine foam in solar-vapor desalination unit after 5 minutes of 1.0 kw·m^{-2} sunlight illumination. (b) The seawater evaporation performance of hydrophobic Fe_3Si aerogel/melamine foam under 1.0 kw·m^{-2} solar illumination.

Table S1. Water evaporation performance comparison of Fe_3Si aerogel/melamine foam and other excellent photothermal materials under sunlight irradiation. The sunlight intensity is around 1000 W m^{-2}.

Materials	Supports	Evaporation rate	ratio (η)	Refs
PVA gel/PPy	none	3.2kg·m^{-2}·h^{-1}	8	1
Hollow carbon	none	1.45kg·m^{-2}·h^{-1}	2.9	2
GO and CNTs	GO/cellulose	1.25kg·m^{-2}·h^{-1}	3.125	3
graphene foam	none	1.4kg·m^{-2}·h^{-1}	3.5	4
Ti_2O_3	cellulose	1.32kg·m^{-2}·h^{-1}	2.6	5
Mg reduced TiO_2	SS mesh	0.8kg·m^{-2}·h^{-1}	1.8	6
Fe_3Si aerogel	none	2.08kg·m^{-2}·h^{-1}	6.71	This work

PVA: poly vinyl alcohol; PPy: polypyrrole; GO: graphene oxide; CNTs: carbon nanotubes; SS: stainless steel.

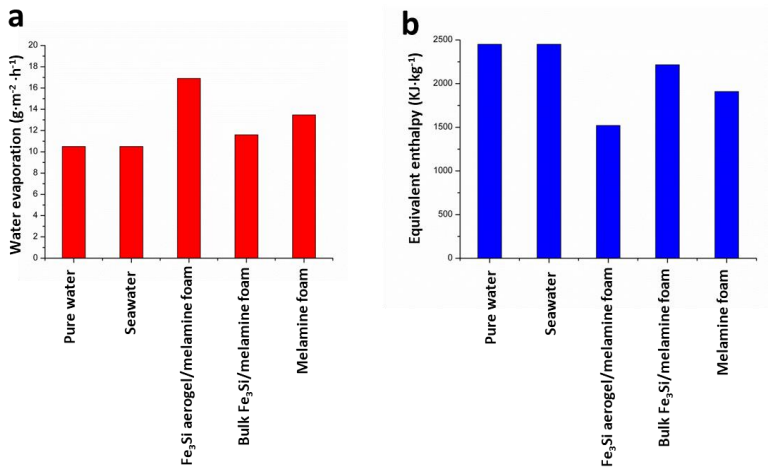

Figure S8. (a) Water evaporation rate under dark circumstances and (b) the corresponding calculated equivalent enthalpy in different conditions.

The calculation is in term of the equation below:

$U = \Delta H_1 * m_1 = \Delta H_2 * m_2$ (eq1)

Where ΔH_1 and m_1 were the evaporation enthalpy and water evaporation rate of pure water under dark circumstances.[1] The different water evaporation cells was put in same dark room at same time under a temperature of 23 ℃, and the value of ΔH_1 was 2450 KJ łkg^{-1}.

Table S2. The seawater evaporation performance comparison of Fe_3Si aerogel, bulk Fe_3Si supported on melamine foam and self-floated Fe_3Si aerogel (S-Fe_3Si aerogel)

Materials	Water evaporation mass for 2 h (kg m^{-2})	Latent heat (kJ/kg)	Temperature increase of water ΔT (k)
Fe_3Si aerogel	4.16	1520	29
Bulk Fe_3Si	2.30	2215	22
S-Fe_3Si aerogel	1.49	2295	61

To assess the effect of low thermal conductivity on the performance of seawater evaporation, the thermal efficiency (η) was calculated in term of the equation below,[1, 7]:

$$\eta = Q_e/Q_s \quad (1)$$

where Q_s is the total solar irradiation energy in three hours, and Q_e is power consumed for seawater vapor generation in three hours, which can be estimated by the following equation,

$$Q_e = m\lambda + mC\Delta T$$

where m is the mass of seawater vapor, λ is the latent heat of the phase change, C is the specific heat capacity of water (4.2 J g^{-1} K^{-1}) and ΔT is the temperature increase of the water. The detailed data for seawater evaporation were shown in Table S2. Fe_3Si aerogel and bulk Fe_3Si supported on melamine foam showed an efficiency of 91.8 % and 70.7 % under the 1.0 kW m^{-2} of solar intensity.

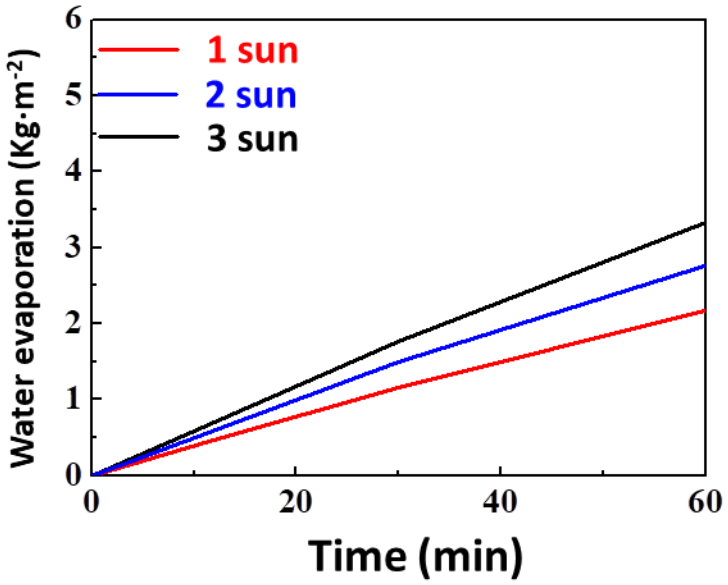

Figure S9. Seawater evaporation performance of Fe_3Si aerogel/melamine foam under 1.0, 2.0 and 3.0 kw·m^{-2} of sunlight irradiation (1 to 3 sun).

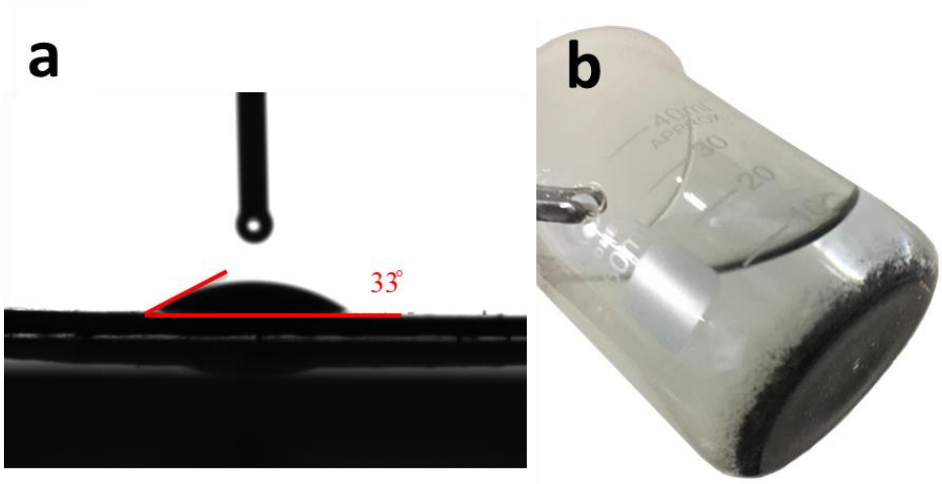

Figure S10. (a) The water contact angle of pristine Fe_3Si aerogel. A water droplet is loaded on the surface of a sample disc, which was prepared by pressing materials. (b) The picture of pristine Fe_3Si aerogel sink in water photographed by camera.

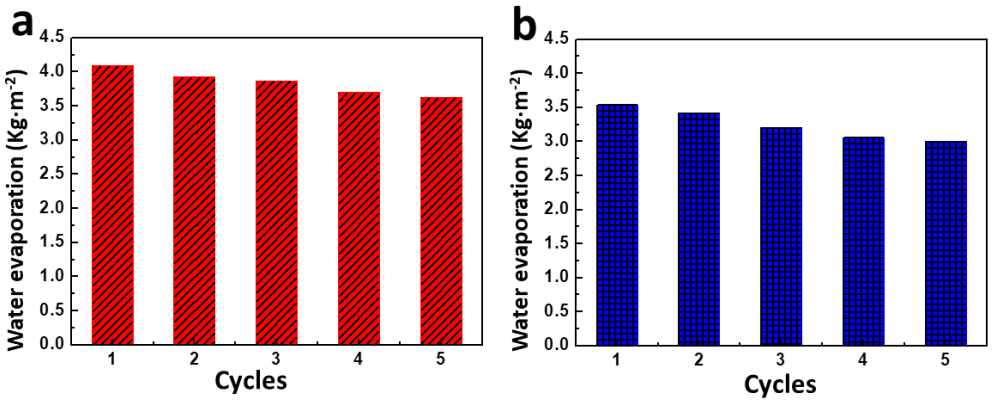

Figure S11. (a, b) The extra five-cycle water evaporation performances of hydrophobic Fe_3Si aerogel floated on 0.5 M H_2SO_4 and 1 M NaOH solutions, respectively, under 1.16 kw·m^{-2} solar illumination. It is revealed that the water evaporation amounts of extra 5 cycles is gradually reduced from 4.05 to 3.55 Kg m^{-2} in 0.5 M H_2SO_4 solution and 3.50 to 3.07 Kg m^{-2} in 1 M NaOH solution, both of which were almost similar to the first five-cycles of water evaporation performance, revealing the excellent stability of hydrophobic Fe_3Si aerogel. The slight decrease of water evaporation rate during cycles test is possibly induced by the residual adsorption of H_2SO_4 and NaOH on Fe_3Si aerogel.

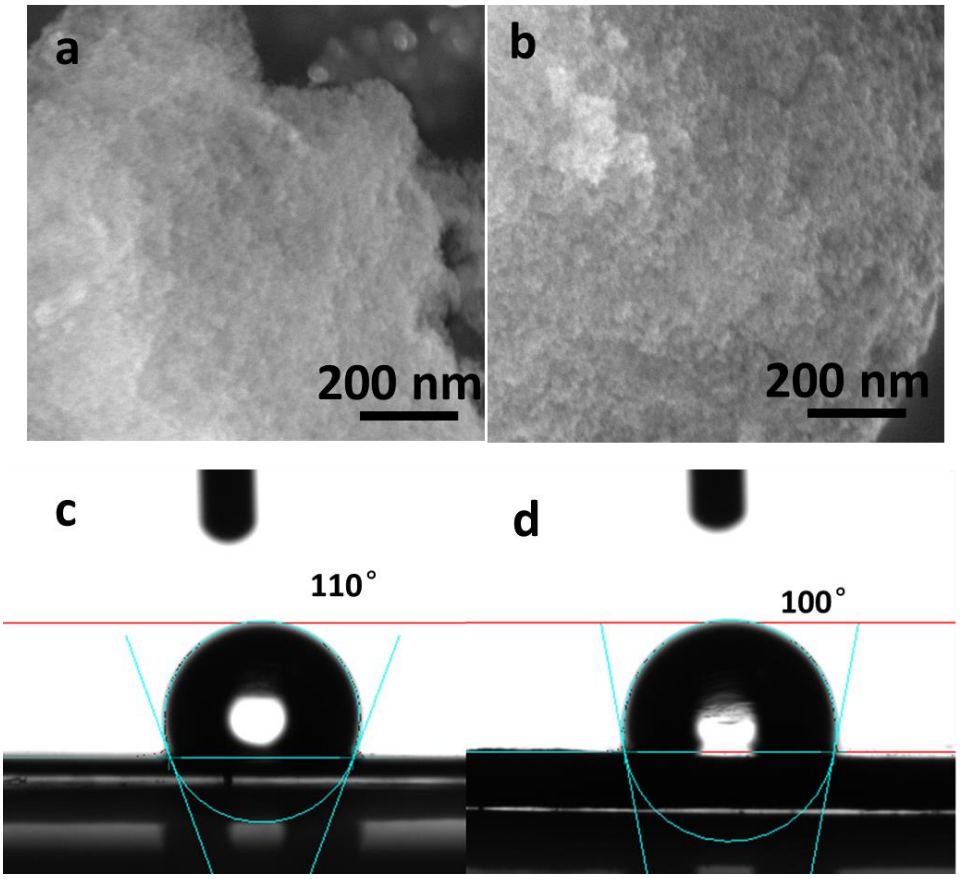

Figure S12. (a, b) SEM images of hydrophobic Fe_3Si aerogel after 10 cycles of photothermal water evaporation form 0.5 M H_2SO_4 and 1 M NaOH, respectively. The SEM images showed that hydrophobic Fe_3Si aerogel still maintained porous structure of pristine Fe_3Si aerogel, without any significant structure degradation. (c, d) Water contact angles of hydrophobic Fe_3Si aerogel after 10 cycles of photothermal water evaporation form 0.5 M H_2SO_4 (contact angel of 110 °) and 1 M NaOH (100 °), respectively. A water droplet is loaded on the surface of a sample disc prepared by pressing materials. In comparison with pristine hydrophobic Fe_3Si aerogel of 110 °, it is suggested that Fe_3Si aerogel was more suitable for photothermal water evaporation from H_2SO_4.

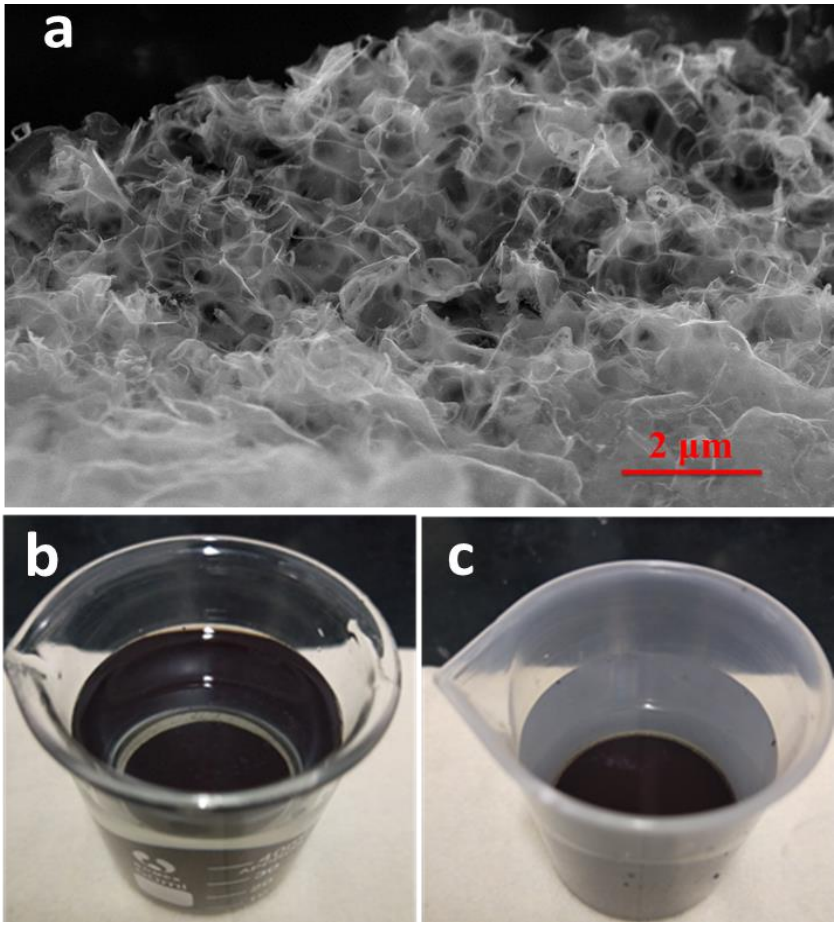

Figure S13. (a) SEM image of porous carbon. (b) and (c) Photographs of porous carbon loaded in 0.5 M H_2SO_4 and 1 M NaOH solutions under 1.16 kw·m^{-2} of sunlight illumination for 1 day. It is clearly seen that, after 1 day, porous carbon was completely deposited at the bottom of H_2SO_4 and NaOH solutions, indicative of unapplicablity for the corosive water evoporation.

Synthesis of porous carbon: 1 g of glucose was dissolved in 5 ml of H_2O, and subsequently added into 20 g of NaCl powder with agitation. After that, the mixture was treated by liquid nitrogen, freeze dried, and annealed in the tube furnace with N_2 atmosphere of 100 sccm at 1000 ℃ for 2 h. Porous carbon was obtained after washing the NaCl with deionized water three times.

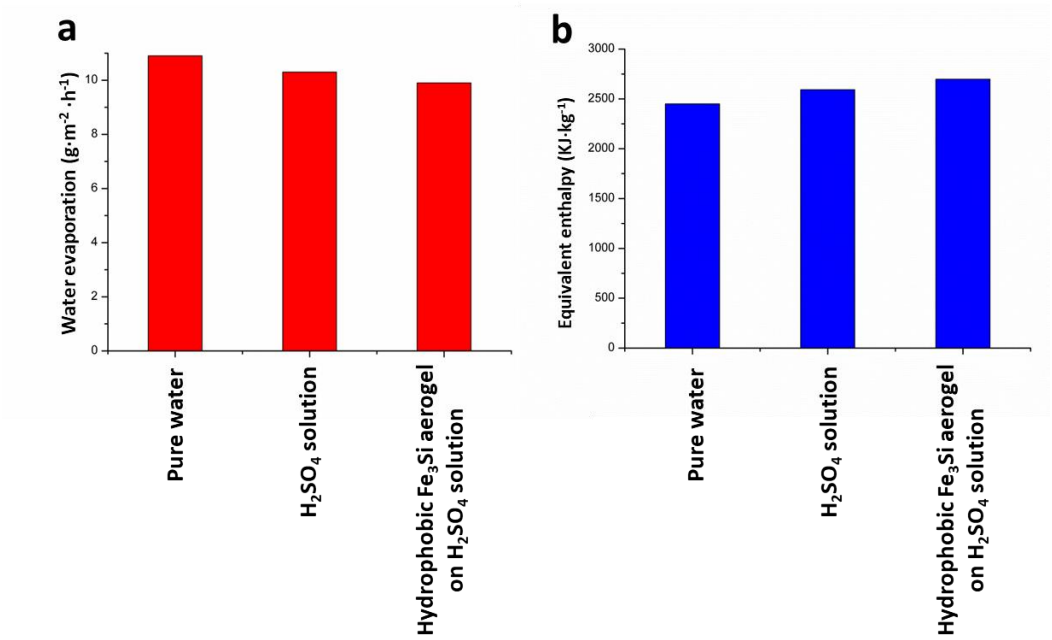

Figure S14. (a) Water evaporation rate under dark circumstances and (b) the corresponding calculated equivalent enthalpy in different conditions of pure water, 0.5 M of H_2SO_4 solution, and hydrophobic Fe_3Si aerogel floated on H_2SO_4 solution. Note that the different water evaporation cells were put in same dark room at same time under a temperature of 18 ℃, and the value of ΔH_1 was 2458 KJ ŀg^{-1} under 18 ℃.

Calculation of Thermal Radiation Power

The heat loss of thermal radiation of Fe_3Si aerogel on seawater, 0.5 M H_2SO_4 and 1 M NaOH solution, respectively, was calculated based on Stefan-Boltzmann law:

$j=\varepsilon\sigma (T_2^4 - T_1^4)$.

Where j is the thermal radiation power, σ is the emissivity, and T is Kelvin temperature (K) of materials. The emissivity was 0.88 for Fe_3Si aerogel. For seawater, 0.5 M H_2SO_4 and 1 M NaOH solution, the ambient temperature was 23, 18, and 18 ℃ (296, 291, 291 K, T_1), respectively, and the temperature of irradiated Fe_3Si aerogel was 52, 84, and 84 ℃ (325, 357, 357 K, T_2), respectively. Therefore, the calculated values j are 0.08, 0.44 and 0.44 KW m^{-2} for seawater, 0.5 M H_2SO_4 and 1M NaOH solution, respectively.

References

1. F. Zhao, X. Zhou, Y. Shi, X. Qian, M. Alexander, X. Zhao, S. Mendez, R. Yang, L. Qu and G. Yu, *Nat. Nanotechnol.*, 2018, **13,** 489–495.
2. J. Zhou, Z. Sun, M. Chen, J. Wang, W. Qiao, D. Long and L. Ling, *Adv. Funct. Mater.*, 2016, **26**, 5368-5375.
3. Y. Li, T. Gao, Z. Yang, C. Chen, W. Luo, J. Song, E. Hitz, C. Jia, Y. Zhou, B. Liu, B. Yang and L. Hu, *Adv. Mater.*, 2017, **29**, 1700981.
4. H. Ren, M. Tang, B. Guan, K. Wang, J. Yang, F. Wang, M. Wang, J. Shan, Z. Chen, D. Wei, H. Peng and Z. Liu, *Adv. Mater.*, 2017, **29**, 1702590.
5. J. Wang, Y. Li, L. Deng, N. Wei, Y. Weng, S. Dong, D. Qi, J. Qiu, X. Chen and T. Wu, *Adv. Mater.*, 2017, **29**, 1603730.
6. M. Ye, J. Jia, Z. Wu, C. Qian, R. Chen, P. G. O'Brien, W. Sun, Y. Dong and G. A. Ozin, *Adv. Energy. Mater.*, 2017, **7**, 1601811.
7. G. Xue, K. Liu, Q. Chen, P. Yang, J. Li, T. Ding, J. Duan, B. Qi and J. Zhou, *ACS. Appl. Mater. Inter.*, 2017, **9**, 15052-15057.